

# The Mass of the Compact Object in the X-Ray Binary 4U 1700-37

M. K. Abubekerov

*Moscow State University, Moscow, Russia*

Received November 17, 2003; in final form, January 9, 2004

**Abstract**—The results of a systematic analysis of master radial-velocity curves for the X-ray binary 4U 1700-37 are presented. The dependence of the mass of the X-ray component on the mass of the optical component is derived in a Roche model based on a fit of the master radial-velocity curve. The parameters of the optical star are used to estimate the mass of the compact object in three ways. The masses derived based on information about the surface gravity of the optical companion and various observational data are  $2.25^{+0.23}_{-0.24}M_{\odot}$  and  $2.14^{+0.50}_{-0.43}M_{\odot}$ . The masses based on the radius of the optical star,  $21.9R_{\odot}$ , are  $1.76^{+0.20}_{-0.21}M_{\odot}$  and  $1.65^{+0.78}_{-0.56}M_{\odot}$ . The mass of the optical component derived from the mass–luminosity relation for X-ray binaries,  $27.4M_{\odot}$ , yields masses for the compact object of  $1.41^{+0.08}_{-0.08}M_{\odot}$  and  $1.35^{+0.18}_{-0.18}M_{\odot}$ . © 2004 MAIK “Nauka/Interperiodica”.

## 1. INTRODUCTION

The X-ray binary 4U 1700-37 was discovered by the UHURU satellite in December 1970 [1]. Subsequent observations revealed eclipses of the X-ray source with a period of 3.412 d. The system was identified with the O6.5Iaf supergiant HD 153919 [2, 3], which displays brightness variations with the same period. The system is 1.8 kpc from the Earth and is made up of a compact object accreting material supplied by an optical companion.

The X-ray radiation of 4U 1700-37 has a hard spectrum that resembles the spectrum of an accreting neutron star [4, 5]. However, no regular pulses associated with the lighthouse effect, which arises during accretion onto a neutron star, are observed. This hinders the construction of a radial-velocity curve for the compact object, and hence determination of the masses of the binary components.

In the early study [6], a least-squares solution for the observed radial-velocity curve was obtained using a model with two point masses. If the mass of the optical component is  $35M_{\odot}$  and the inclination of the orbit is  $90^{\circ}$ , the mass of the compact object yielded by this model is  $2.4M_{\odot}$ .

Heap and Corcoran [7] estimated the masses of the binary components using the algorithm of [8] together with information about the duration of the eclipses and the radius of the optical component. Based on a mass for the optical component of  $52 \pm 2M_{\odot}$ , they obtained a mass for the compact object of  $1.8 \pm 0.4M_{\odot}$ . An earlier analysis carried out using the same method [9] yielded a mass for the relativistic component of  $1.3M_{\odot}$  for a mass of the optical component of  $27M_{\odot}$ .

The Monte-Carlo method used by Jones [10] yields a mass for the compact object of  $2.6^{+2.3}_{-1.4}M_{\odot}$  for a mass of the optical component of  $30^{+11}_{-7}M_{\odot}$ .

Clark [11], who also used a Monte-Carlo method, derived a mass for the compact object of  $2.44 \pm 0.27M_{\odot}$  for a mass of the optical companion of  $58 \pm 11M_{\odot}$ . The modeling in this particular study was not carried out entirely correctly. In place of the half-amplitude of the radial-velocity curve for the optical component,  $K_v = 18.7 \pm 1.0$  km/s, corresponding to a circular orbit, Clark [11] used the value  $K_v = 20.6 \pm 1.0$  km/s, leading to a slight overestimation of the mass of the compact object.

The uncertainty in the estimated mass of the X-ray component of the binary 4U 1700-37 is obvious. Let us consider the factors hindering accurate estimation of the mass of the relativistic component in this binary system.

First, uncertainty in the mass of the relativistic component in 4U 1700-37 is due to the unknown mass of the optical component, which has only been determined from its spectral type and luminosity class with comparatively large uncertainties.

Second, the Monte-Carlo method used for the mass estimates, as well as the method of [7, 9], relied on relations obtained for a point-mass formalism. Models approximating the O supergiant as a point mass of electromagnetic radiation do not take into account a wide range of phenomena associated with the interaction between the components. Therefore, a correct estimation of the mass of the relativistic component is not possible using this type of model,

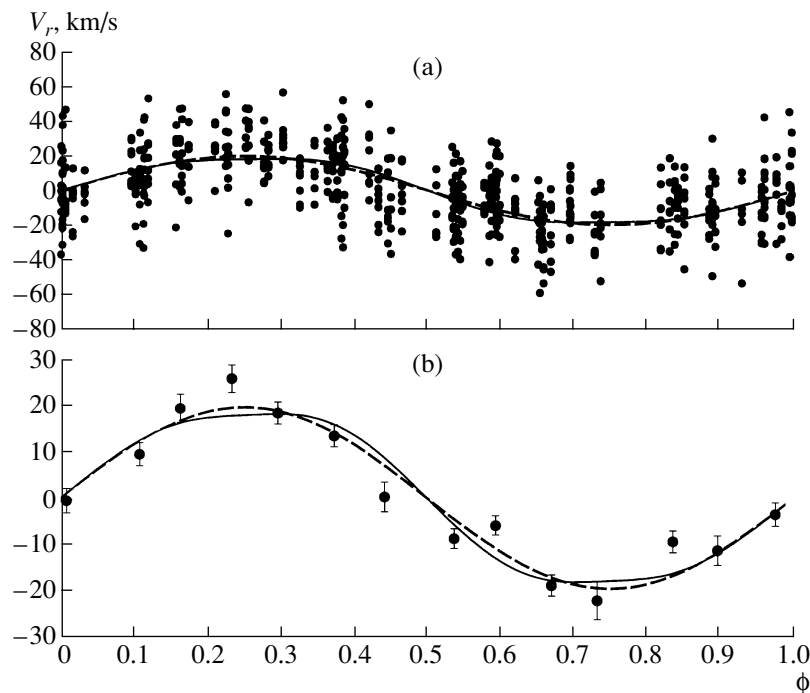


**Fig. 1.** (a) Master observed radial-velocity curve for the close X-ray binary 4U 1700-37. The filled circles show the radial velocities derived from hydrogen absorption lines [12]. For comparison, we also show theoretical radial-velocity curves for a Roche model (solid) and point-mass model (dashed) for  $m_x = 2.11M_\odot$ , corresponding to the minimum residual in the Roche model with  $m_v = 50M_\odot$  computed using method 2 (excluding the mean radial velocities at phases 0.4–0.6). The parameters of the Roche model are presented in Table 1. (b) Radial velocities averaged within phase intervals (filled circles show the mean radial velocities within given phase bins). For comparison, we also show theoretical radial-velocity curves for the Roche model (solid) and point-mass model (dashed) for  $m_x = 2.11M_\odot$  and  $m_v = 50M_\odot$ .

even if the mass of the optical component is precisely known.

Third, the Monte-Carlo method uses the half-amplitude of the radial-velocity curve of the optical component (which is known only to within  $\sim 5\text{--}10\%$ ), ignoring information contained in the shape of this curve.

It is clear that the collected spectroscopic observations must be interpreted using a more realistic model. A correct estimation of the masses of the components in 4U 1700-37 will represent another step forward in our understanding of the nature of the X-ray source.

## 2. OBSERVATIONAL MATERIAL

We used the data of [12, 13] to construct a master radial-velocity curve, adopting the center of the eclipse of the X-ray source by the optical component as the zero phase in both cases.

The spectral data of [12] were obtained in 1973–1976 on the 152-cm telescope of the European Southern Observatory. The radial velocities were determined from the H $\beta$ , H $\gamma$ , H $\delta$ , H8, H9, H10, H11, and H12 hydrogen Balmer absorption lines.

The radial velocities were measured in terms of the absolute shift of the absorption-line core relative to its laboratory wavelength. Therefore, we needed to correct the spectral data for the systemic velocity before using them in the master radial-velocity curve.

Note that the systemic velocity of the stellar system determined from the hydrogen Balmer absorption lines grows with decreasing line number in the series—the so-called Balmer progression [14, 15]. For example, the systemic radial velocities for the H $\delta$ , H $\gamma$ , and H $\beta$  lines are  $-82.7$ ,  $-110.3$ , and  $-152.2$  km/s, respectively. The increase in the systemic radial velocity with decreasing line number in the series of absorption lines is associated with the fact that the cores of the lines at the beginning of the series are formed in higher layers of the stellar atmosphere, where a radial outflow has already developed in the form of a stellar wind. The systemic velocities obtained using the higher-order Balmer H10, H11, and H12 absorption lines are  $-72.7$ ,  $-83.3$ , and  $-78.4$  km/s, respectively. Since these lines form at the base of the photosphere of the optical star and do not experience strong perturbation by the stellar wind, their mean value,  $-78.1$  km/s, can be considered to be the  $\gamma$  velocity of the 4U 1700-37 system.

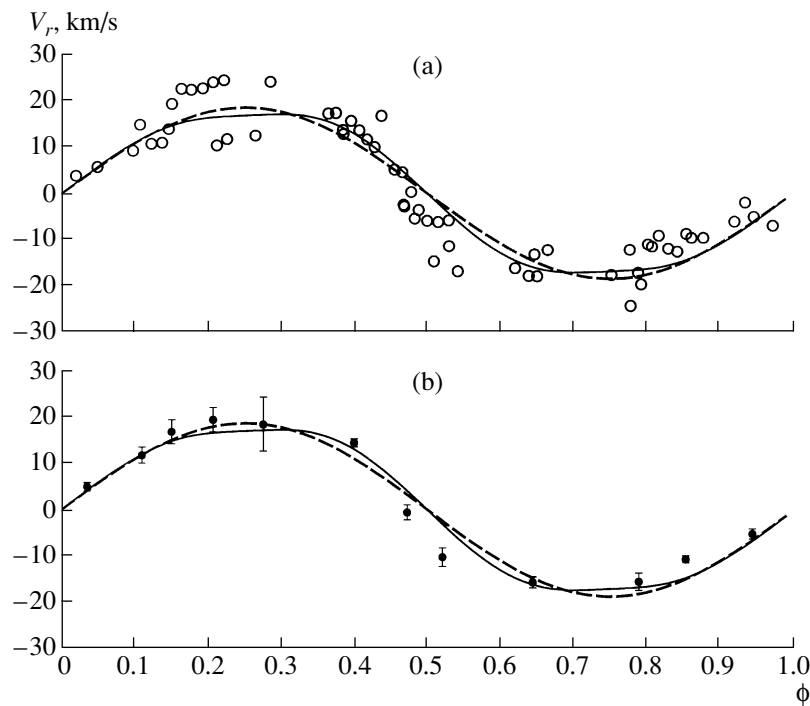


**Fig. 2.** (a) Same as Fig. 1a, but with open circles showing radial velocities determined from the IUE spectral data of [13] and theoretical radial-velocity curves shown for  $m_x = 2.01M_\odot$  and  $m_v = 50M_\odot$ . (b) Same as Fig. 1b, but with theoretical radial-velocity curves shown for  $m_x = 2.01M_\odot$  and  $m_v = 50M_\odot$ .

The data of [12] gave us 570 radial-velocity values distributed approximately uniformly in phase. The master radial-velocity curve is presented in Fig. 1a.

The IUE satellite has taken more than 60 spectra of 4U 1700-37. The results of these high-accuracy spectral observations are presented in [13]. The radial-velocity measurements in this case were obtained by cross-correlating intervals of the spectrum in the range 1300–1850Å. The data of [13] gave us 61 radial-velocities; the corresponding radial-velocity curve is presented in Fig. 2a.

The complex processes occurring at the surface of the optical component and in various gaseous structures in the binary hinder determination of the intrinsic radial velocity of the optical component. The observed radial velocities are unavoidably distorted by random errors. We averaged the radial velocities within phase intervals in order to decrease the influence of such random errors. These mean observed radial-velocity curves are presented in Figs. 1b and 2b. Note that, in light of the recent study [16], the errors introduced to the observed radial velocity of the optical star by tidal–gravitational waves should also be random, and can be suppressed by averaging over many nights of observations.

### 3. INTERPRETATION OF THE RADIAL-VELOCITY CURVES

The optical component in the close binary 4U 1700-37 is close to filling its critical Roche lobe [17]. Due to the tidal action of the relativistic component, the shape of the optical star is not spherical. The side facing the relativistic component is heated by X-ray radiation from this star. These effects associated with the interaction of the components must be taken into consideration when interpreting the observed radial-velocity curve of 4U 1700-37. Therefore, the mean radial velocities should be interpreted using a Roche model, thereby making it possible in a first approximation to include these effects. A detailed description of the Roche model is given in [18, 19], and we do not present this information again here. The numerical values of the Roche-model parameters for 4U 1700-37 are presented in Table 1.

The masses of both components were treated as unknown parameters. Since the process of finding a best fit is fairly cumbersome in this case, we adopted an approach in which we carried out a series of exhaustive parameter searches. For each mass of the optical component from the discrete set  $m_v = 20, 30, 40, 50, 58,$  and  $70M_\odot$ , we carried out an exhaustive search for the optimum mass of the compact object,  $m_x$ . This process yielded a

**Table 1.** Numerical values of parameters used to synthesize radial-velocity curves for 4U 1700-37 in the Roche model

$P$ , days	3.411581	Period
$e$	0.0	Eccentricity
$\omega$ , deg.	0.0	Longitude of periastron of the optical component
$i$ , deg.	67*	Orbital inclination
$\mu$	0.93*	Roche-lobe filling factor for the optical component at periastron
$f$	0.9	Rotation-asynchronization coefficient
$T_{\text{eff}}$ , K	36 000**	Effective temperature of the optical component
$\beta$	0.25	Gravitational-darkening coefficient
$k_x$	0.0005	Ratio of the X-ray luminosity of the relativistic component to the bolometric luminosity of the optical component, $L_x/L_v$
$A$	0.5	Coefficient for reprocessing of the X-ray radiation
$u$	0.3***	Limb-darkening coefficient

\* Data taken from [17].

\*\* Data taken from [11].

\*\*\* Data taken from [20].

relationship between the masses of the compact and optical components.

The residual between the mean observed radial-velocity curve and the theoretical curve was calculated using the formula

$$\Delta(m_x) = \frac{\sum_{j=1}^M (n_j - 1) \sum_{j=1}^M n_j (V_j^{\text{teor}} - \bar{V}_j^{\text{obs}})^2}{M \sum_{j=1}^M n_j (n_j - 1) \sigma_j^2}, \quad (1)$$

where  $\bar{V}_j^{\text{obs}}$  is the observed mean radial velocity in a phase interval centered on phase  $\bar{\phi}_j$ ,  $V_j^{\text{teor}}$  the theoretical radial velocity at this phase,  $\sigma_j$  the rms deviation of  $\bar{V}_j^{\text{obs}}$  from the observed radial velocities in the phase interval centered on phase  $\bar{\phi}_j$ ,  $M$  the number of phase intervals, and  $n_j$  the number of averaged observed radial velocities in this phase interval.

The quantity  $\Delta(m_x)$  is distributed according to a Fisher law,  $F_{M, \sum_{j=1}^M (n_j - 1), \alpha}$  [21]. We can therefore find

the confidence set for the parameter  $m_x$  for a given value of  $m_v$  corresponding to a specified significance level  $\alpha$ . This consists of the three values of  $m_x$  for which

$$\Delta(m_x) \leq F_{M, \sum_{j=1}^M (n_j - 1), \alpha}.$$

We obtained fits for both a Roche model and a point-mass model. The latter model served to identify

divergences of the two model results. The fitting of the mean radial-velocity curve was carried out separately for the spectral data of [12] and [13].

We should say a few words about the stellar wind of the optical component in the 4U 1700-37 system. The optical star is an O supergiant. Non-uniformity in the gravitational forces at its surface and heating of the surface facing the relativistic companion disrupts the isotropy of the stellar-wind outflow. The wind speed near the Lagrange point  $L_1$  grows, manifest as an excess negative radial velocity near phase 0.5 (when the X-ray source is in front of the O supergiant; Figs. 1b and 2b). The anisotropy of the stellar wind introduces systematic errors in the observed radial-velocity curve. Therefore, we obtained fits to the mean observed radial-velocity curves in two ways:

*Method 1.* Using all the mean observed radial velocities.

*Method 2.* Excluding the mean observed radial velocities at phases 0.4–0.6, where the distorting effect of the anisotropic stellar wind is strongest.

We chose the 5% significance level as the critical level for our work. The fits obtained for the spectral data of [12, 13] using method 1 were not acceptable at this level for either the Roche model or the point-mass model. The behavior of the residuals for the Roche-model fit to the data of [12, 13] are presented in Figs. 3a and 3b. It is not possible to construct a relation between the masses of the components in this case.

Fitting the mean observed radial velocities while indirectly taking into account the anisotropy of the

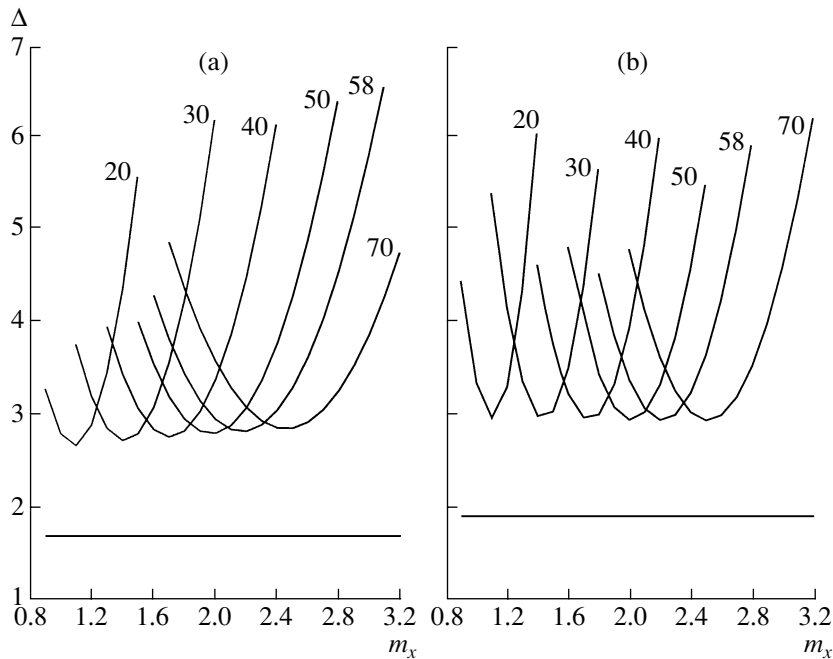


**Fig. 3.** (a) Residuals between the mean observed radial-velocity curve for 4U 1700-37 for the data of [12] and the curve synthesized in the Roche model, obtained using method 1 (i.e., using all of the mean radial velocities). The horizontal line corresponds to the critical Fisher criterion  $\Delta_{14,570} = 1.69$  for the 5% significance level. The masses of the optical component in solar masses for which the residuals were obtained are indicated near the curves. (b) Same for the data of [13]. The horizontal line corresponds to the critical Fisher criterion  $\Delta_{12,61} = 1.916$  for the 5% level.

wind (method 2) enabled us to obtain an acceptable model at the 5% significance level. This indicates the importance of including the anisotropy of the stellar wind when interpreting the radial-velocity curves of OB stars in close binary systems [22]. Figures 4a and 4b show the residuals obtained for the Roche-model fits to the mean observed radial-velocity curves. We used the results of these fits to construct the dependence of the mass of the X-ray component on the mass of the optical component (Figs. 5a and 5b). For a mass of the optical component of  $69M_{\odot}$ , the minimum residual in the analysis using the data of [12], achieved for  $m_x = 2.61M_{\odot}$ , is equal to the quantile. Therefore, the error corridor for the component-mass dependence in Fig. 5a is cut off at  $m_v = 69M_{\odot}$ . The numerical results of our fitting of the data of [12] and [13] using point-mass and Roche models are given in Tables 2 and 3.

We can see from these tables that the masses of the compact object obtained in the Roche and point-mass models are similar. This can be explained in two ways. First, due to the small gravitational force near the Lagrange point  $L_1$ , the temperature of the “nose” of the optical star is lower than that of its remaining surface (gravitational darkening). Second, the heating of the part of the optical star facing the X-ray source is very low ( $k_x = 0.0005$ ). Therefore, the contribution of the “nose,” which introduces the largest

perturbations into the observed radial-velocity curve, to the integrated radiation of the optical component is small. The similarity of the results for the Roche and point-mass models comes about because radiation of the optical component is dominated by the spherically symmetric part of its surface. The influence of the heating coefficient on the shape of the radial-velocity curve is discussed in more detail in [18].

The relations between the masses of the optical and X-ray components obtained using the data of [12] and [13] are in good agreement with each other (Figs. 5a and 5b, Tables 2 and 3).

Because the orbital inclination is not accurately known, we also obtained fits applying method 2 to the spectral data of [13] for inclinations of  $62^{\circ}$  and  $72^{\circ}$ , with the remaining parameters for the Roche model taken to be the same as before (Table 1). The numerical results are presented in column 1 in Tables 4 and 5, and the results are shown graphically in Figs. 6a and 6b.

The dependence of the mass of the compact object on the orbital inclination in the point-mass model is given by the relation  $m_v \sim \sin^{-3} i$ . We carried out a test similar to that of [23] to verify how accurately this relation was obeyed for the Roche model.

The mass of the compact object derived in the Roche model for an orbital inclination  $i = 67^{\circ}$  was

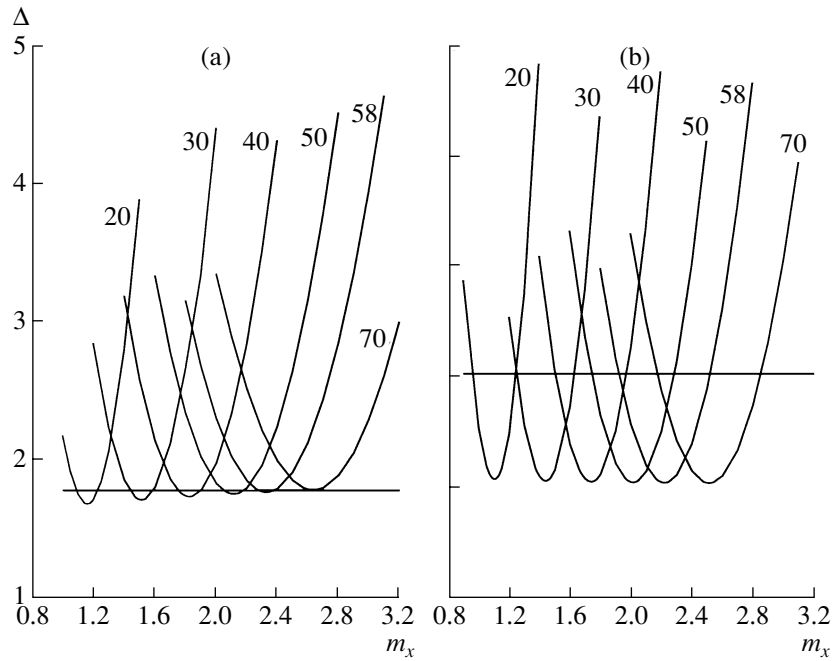


**Fig. 4.** (a) Residuals between the mean observed radial-velocity curve for 4U 1700-37 for the data of [12] and the curve synthesized in the Roche model, obtained using method 2 (i.e., excluding the mean radial velocities at phases 0.4–0.6). The horizontal line corresponds to the critical Fisher criterion  $\Delta_{11,428} = 1.79$  for the 5% significance level. The masses of the optical component in solar masses for which the residuals were obtained are indicated near the curves. (b) Same for the data of [13]. The horizontal line corresponds to the critical Fisher criterion  $\Delta_{10,48} = 2.03$  for the 5% level.

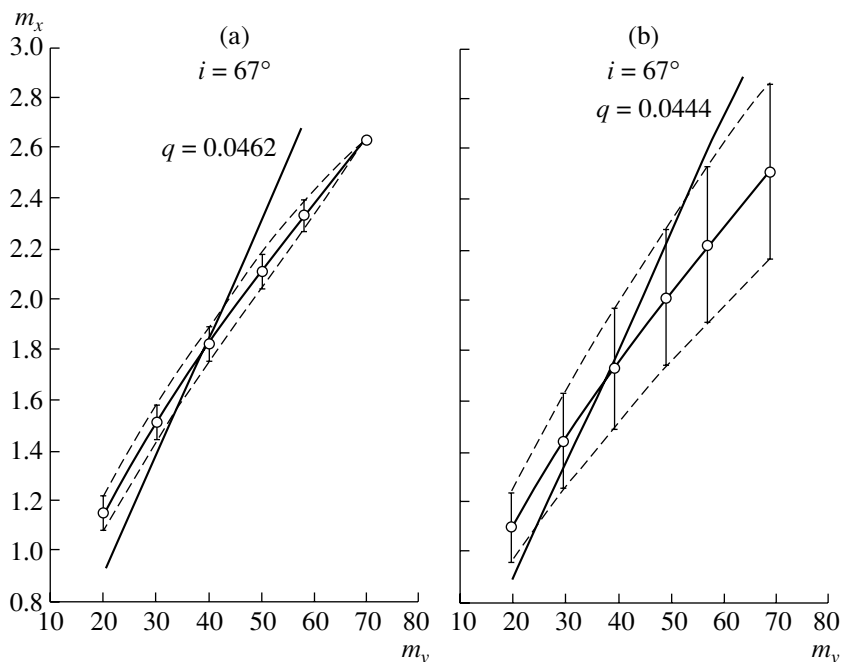


**Fig. 5.** (a) Dependence of the mass of the compact object in 4U 1700-37 on the mass of the optical star for an orbital inclination of  $67^\circ$ . The fit was obtained in a Roche model for the radial velocities determined from hydrogen Balmer absorption lines in [12] using method 2 (i.e., excluding the mean radial velocities at phases 0.4–0.6). The line corresponds to the relation between  $m_x$  and  $m_v$  for the component-mass ratio  $q = 0.0462$  found from (4). (b) Same for the IUE data of [13]. The line corresponds to the relation between  $m_x$  and  $m_v$  for the component-mass ratio  $q = 0.0444$  found from (4).

**Table 2.** Mass of the relativistic component of 4U 1700-37 obtained from the fit of the data of [12] in Roche (“R”) and point-mass (“P”) models

$m_v, M_\odot$	$m_x(\text{P}), M_\odot$	$m_x(\text{R}), M_\odot$
20	$1.15^{+0.13}_{-0.12}$	$1.15^{+0.08}_{-0.06}$
30	$1.51^{+0.16}_{-0.16}$	$1.51^{+0.08}_{-0.07}$
40	$1.82^{+0.20}_{-0.20}$	$1.82^{+0.08}_{-0.07}$
50	$2.11^{+0.23}_{-0.23}$	$2.11^{+0.07}_{-0.06}$
58	$2.32^{+0.26}_{-0.25}$	$2.33^{+0.05}_{-0.06}$
70	$2.64^{+0.28}_{-0.30}$	$2.64^*$

\* Confidence interval not indicated, since the model is rejected at the 5% significance level.

recalculated for  $i = 62^\circ$  and  $i = 72^\circ$  using formulas (2) and (3):

$$m_x(62^\circ) = m_x(67^\circ) \frac{\sin^3 67^\circ}{\sin^3 62^\circ}, \quad (2)$$

$$m_x(72^\circ) = m_x(67^\circ) \frac{\sin^3 67^\circ}{\sin^3 72^\circ}. \quad (3)$$

Here,  $m_x(62^\circ)$ ,  $m_x(67^\circ)$ , and  $m_x(72^\circ)$  are the masses of the relativistic component for inclinations of  $62^\circ$ ,  $67^\circ$ , and  $72^\circ$ . The results of recalculating the mass of the compact object using (2) and (3) are presented in the second columns of Tables 4 and 5.

A comparison of the first and second columns in Tables 4 and 5 shows that the relation  $m_v \sim \sin^{-3}i$  yields results that are close to, but not strictly coincident with, those for the Roche model. Nevertheless, the masses agree within the errors (Figs. 6a, 6b). Therefore, if the inclination  $i$  is refined, the mass of the compact object  $m_x$  can be approximately recalculated using the relation  $m_x \sim \sin^{-3}i$ . A more precise determination of the component masses for specified values of  $i$  can be carried out by interpolating the results of Tables 2–5 (see also Figs. 5 and

#### 4. DETERMINATION OF THE COMPONENT MASSES

##### *Based on the Gravitational Acceleration of the Optical Component*

A detailed non-LTE analysis of spectra of the optical star in the 4U 1700-37 system was carried out in [11]. The gravitational acceleration  $\log g$  derived from the wings of Balmer and HeI absorption lines in the spectrum of the optical component, HD 153919, lies in the range 3.45–3.55 [11]. The bolometric luminosity and effective temperature of the optical component were found to be  $\log(L/L_\odot) = 5.82$  and

**Table 3.** Mass of the relativistic component of 4U 1700-37 obtained from the fit of the data of [13] in Roche (“R”) and point-mass (“P”) models

$m_v, M_\odot$	$m_x(\text{P}), M_\odot$	$m_x(\text{R}), M_\odot$
20	$1.09^{+0.10}_{-0.10}$	$1.10^{+0.15}_{-0.14}$
30	$1.42^{+0.13}_{-0.13}$	$1.44^{+0.19}_{-0.19}$
40	$1.72^{+0.16}_{-0.16}$	$1.73^{+0.25}_{-0.23}$
50	$1.99^{+0.18}_{-0.19}$	$2.01^{+0.28}_{-0.27}$
58	$2.19^{+0.21}_{-0.20}$	$2.22^{+0.31}_{-0.31}$
70	$2.49^{+0.23}_{-0.24}$	$2.51^{+0.35}_{-0.34}$

$35\,000 \pm 1000$  K, yielding a radius of  $21.9R_\odot$ . Using the values  $\log g = 3.45 - 3.55$  and  $R_v = 21.9R_\odot$ , we obtain a lower limit for the mass of the optical star of  $55^{+7}_-6M_\odot$ . The mass of the optical star derived from the observed free-fall acceleration will be a lower limit, since the true acceleration will be greater due to the action of centrifugal forces. Clark [11] suggested that the lower limit for the mass of the optical star is close to  $50M_\odot$ , while the upper limit, derived from the position of HD 153919 in the Hertzsprung–Russell diagram, is no more than  $60M_\odot$ . The mass of the compact object corresponding to a mass for the optical star of  $55^{+7}_-6M_\odot$  and an inclination of  $67^\circ$  based on the relation between the component masses constructed using the spectral data of [12] is  $2.25^{+0.23}_{-0.24}M_\odot$  (Fig. 5a). The relation between the component masses constructed for the IUE spectral data of [13] yields a mass for the relativistic component of  $2.14^{+0.50}_{-0.43}M_\odot$  (Fig. 5b).

The masses of the relativistic component obtained from the component-mass relation based on the IUE spectral data of [13] are  $2.26^{+0.49}_{-0.44}M_\odot$  and  $2.06^{+0.47}_{-0.39}M_\odot$  for inclinations of  $62^\circ$  and  $72^\circ$ , respectively (Fig. 6b).

##### *Based on the Radius of the Optical Component*

The radius of the optical component  $R_v$ , Roche-lobe filling factor  $\mu$ , eccentricity  $e$ , inclination  $i$ , orbital period  $P$ , mass function for the optical component  $f_v(m)$ , and component-mass ratio  $q = m_x/m_v$  are related by (4) (see, for example, [17]):

$$\sin i = \frac{0.38\mu}{R_v} \left( \frac{GP^2 f_v(m)}{4\pi^2} \right)^{1/3} \frac{1+q}{q^{1.208}}, \quad (4)$$

where  $f_v(m)$  is defined to be

$$f_v(m) = \frac{P(1-e^2)^{3/2}}{2\pi G} K_v^3.$$

**Table 4.** Column 1: Mass of the relativistic component obtained for the Roche model, method 2, the data of [13], and orbital inclination  $i = 62^\circ$ . Column 2: Result of using (2) to recalculate the mass of the compact object obtained for the Roche model and  $i = 67^\circ$  (see text for details)

$m_v, M_\odot$	$m_x, M_\odot$	
	1	2
20	$1.16^{+0.15}_{-0.15}$	1.25
30	$1.51^{+0.20}_{-0.20}$	1.63
40	$1.82^{+0.24}_{-0.24}$	1.96
50	$2.11^{+0.28}_{-0.28}$	2.28
58	$2.33^{+0.30}_{-0.31}$	2.52
70	$2.63^{+0.35}_{-0.34}$	2.84

**Table 5.** Column 1: Mass of the relativistic component obtained for the Roche model, method 2, the data of [13], and orbital inclination  $i = 62^\circ$ . Column 2: Result of using (3) to recalculate the mass of the compact object obtained for the Roche model and  $i = 67^\circ$  (see text for details)

$m_v, M_\odot$	$m_x, M_\odot$	
	1	2
20	$1.06^{+0.15}_{-0.14}$	1.00
30	$1.39^{+0.19}_{-0.20}$	1.31
40	$1.67^{+0.24}_{-0.23}$	1.57
50	$1.94^{+0.27}_{-0.27}$	1.82
58	$2.13^{+0.30}_{-0.29}$	2.01
70	$2.51^{+0.33}_{-0.33}$	2.28

Consequently, if we have information about the radius of the optical component and the remaining parameters of the binary system in (4), we can determine the component-mass ratio  $q$ .

The values for  $\mu$ ,  $e$ ,  $P$ , and  $i$  were taken from Table 1. We carried out a search for the velocity of the center of mass of the optical component  $K_v$  in a point-mass model. We constructed a radial-velocity curve for a point-mass model for each pair of component masses determined in the Roche model (Tables 2 and 3). Further, we determined the mean value of  $K_v$ . The results for the spectral data of [12] and [13] were  $K_v = 19.72 \pm 0.02$  km/s and  $K_v = 18.81 \pm 0.01$  km/s, respectively.

We can obtain an equation for  $q$  by substituting the radius of the optical star  $R_v = 21.9R_\odot$  [11] into (4). Solution of (4) using the value  $K_v = 19.72$  km/s based on the data of [12] yields the component-mass

ratio  $q = 0.0462$ ; using the value  $K_v = 18.81$  km/s based on the data of [13] yields  $q = 0.0444$ .

We show the corresponding curves on the component-mass relations in Figs. 5a and 5b. The intersection of a line with the region of allowed masses identifies the corresponding mass of the compact object. The resulting masses for the relativistic component based on the data of [12] and [13] are  $1.76^{+0.20}_{-0.21}M_\odot$  (Fig. 5a) and  $1.65^{+0.78}_{-0.56}M_\odot$  (Fig. 5b).

#### Based on the Mass–Luminosity Relation

The mass of the optical component determined from the mean linear mass–luminosity relation for main-sequence stars in non-interacting binaries is  $49.5M_\odot$  [24]. Using the relations between the component masses based on the data of [12] and [13], this value corresponds to masses for the compact object of  $2.08^{+0.07}_{-0.07}M_\odot$  (Fig. 5a) and  $1.98^{+0.27}_{-0.26}M_\odot$  (Fig. 5b).

However, the mass–luminosity relation for the optical components of X-ray binaries differs from the analogous relation for single stars [25]. When the Roche lobe is filled or there is an intense stellar wind, the optical star in a close binary loses the upper layers of its atmosphere, so that the temperature of its surface and its luminosity are higher than for an isolated star of the same mass. The observed overabundances of carbon and nitrogen on the surface of the optical star in the 4U 1700–37 system [11] confirm that this star has lost the upper layers of its atmosphere. Figure 7 presents a mass–luminosity relation for OB stars in X-ray binaries based on the data of [26] and [27]. We can see that the luminosity of the optical component,  $\log(L/L_\odot) = 5.82$  [11], corresponds to a mass of  $27.4M_\odot$ . For this mass, the masses of the relativistic component that are implied by the component-mass relations constructed using the data of [12] and [13] are  $1.41^{+0.08}_{-0.08}M_\odot$  (Fig. 5a) and  $1.35^{+0.18}_{-0.18}M_\odot$  (Fig. 5b).

Thus, based on the mass–luminosity relation for OB stars in X-ray binaries, the mass of the relativistic object in the 4U 1700–37 system agrees within the errors with the mean mass of neutron stars,  $1.35^{+0.04}_{-0.04}M_\odot$  [28].

## 5. CONCLUSION

Our main result is the relationships between the masses of the optical and relativistic components in the X-ray binary system 4U 1700–37 obtained for orbital inclinations  $i = 62^\circ$ ,  $67^\circ$ , and  $72^\circ$  (Figs. 5 and 6). We have also estimated the mass of the compact object in 4U 1700–37 based on the known parameters of the optical component. It has not been conclusively demonstrated whether the compact object in

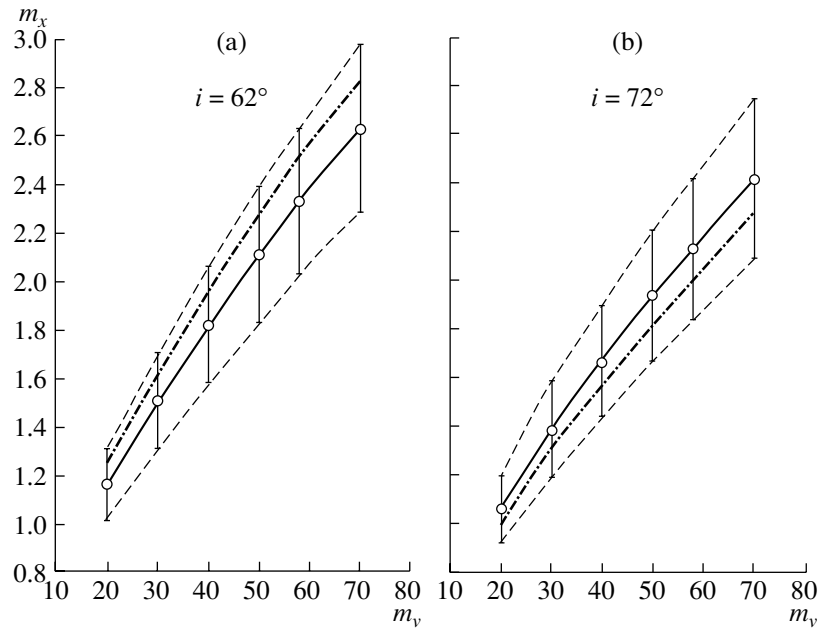


**Fig. 6.** (a) Dependence of the mass of the compact object in 4U 1700-37 on the mass of the optical star for  $i = 62^\circ$ . The fit was obtained for the Roche model for the data of [13] using method 2 (i.e., excluding observed radial velocities at phases 0.4–0.6). The dot–dashed line corresponds to the masses of the compact object obtained by using (2) to recalculate the masses obtained for the Roche model and  $i = 67^\circ$ . (b) Same for  $i = 72^\circ$ . The dot–dashed line corresponds to the masses of the compact object obtained by using (3) to recalculate the masses obtained for the Roche model and  $i = 67^\circ$ .

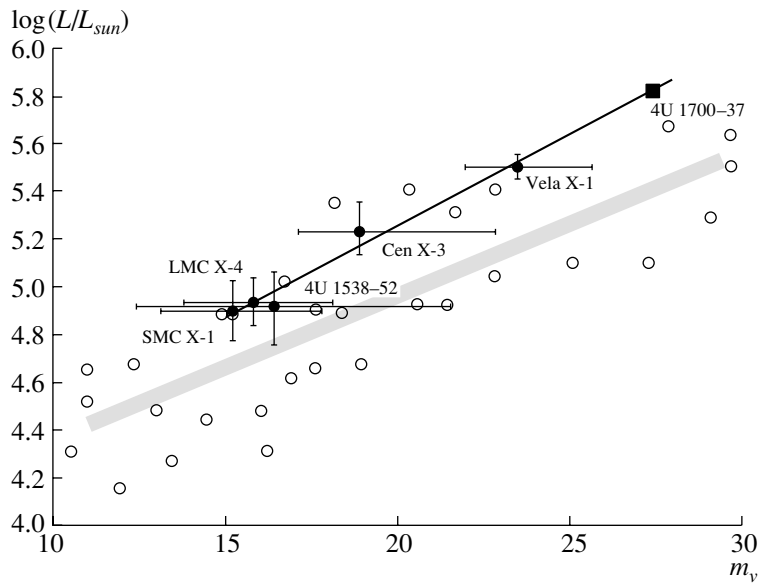


**Fig. 7.** Mass–luminosity relation for OB supergiants in X-ray binary systems (thin, dark line). The filled circles mark the positions of OB giants according to the data of [26, 27], with the names of the X-ray binary systems indicated nearby. The filled square marks the position of the optical component of the 4U 1700-37 system based on the luminosity  $\log(L/L_\odot) = 5.82$  [11]. The hollow circles mark the positions of OB supergiants in non-interacting binaries on the mass–luminosity relation according to the data of [24]; the wide, grey line shows a least-squares linear approximation to this relation.

the 4U 1700-37 system is a low-mass black hole or a neutron star. Our results support the idea that it is a neutron star.

The masses for the relativistic component obtained using the mass–luminosity relation for OB stars in X-ray binaries are  $1.41^{+0.08}_{-0.08} M_\odot$  and

$1.35_{-0.18}^{+0.18} M_{\odot}$ , which agrees within the errors with the mean mass of neutron stars,  $1.35_{-0.04}^{+0.04} M_{\odot}$  [28]. The masses of the compact object obtained based on the surface gravitational acceleration of the optical component are  $2.25_{-0.24}^{+0.23} M_{\odot}$  and  $2.14_{-0.43}^{+0.50} M_{\odot}$ , while those based on the radius of the optical component are  $1.76_{-0.21}^{+0.20} M_{\odot}$  and  $1.65_{-0.56}^{+0.78} M_{\odot}$ . These estimates for the mass of the compact object in 4U 1700-37 coincide within the errors with the mass of the Vela X-1 X-ray pulsar,  $1.93_{-0.21}^{+0.19} M_{\odot}$  [23]. It may be that, similar to the situation with Vela X-1, the compact object in 4U 1700-37 is a massive neutron star. The hard X-ray spectrum of 4U 1700-37, which resembles the spectra of X-ray pulsars [4, 5], also provides evidence that the compact object is a neutron star. The absence of periodic X-ray pulsar from 4U 1700-37 associated with the rotation of an accreting neutron star can be understood if the magnetic-dipole axis and rotational axis are coincident.

It is not currently possible to give an unambiguous estimate of the mass of the relativistic component in 4U 1700-37. Additional information about the optical component is required to refine the mass of the relativistic component. For example, the space astrometric project GAIA planned by the European Southern Observatory will measure the trigonometric parallaxes and distances to millions of stars in the Galaxy. Knowledge of the distance to the 4U 1700-37 system will make it possible to obtain a direct estimate of the radius of the optical star, which can, in turn, be used to derive a trustworthy estimate of the mass of the compact object. Further careful searches for phenomena associated with the possible presence of an X-ray pulsar in 4U 1700-37 can also play an important role in elucidating the nature of this system.

#### ACKNOWLEDGMENTS

This work was supported by a grant from the program "Leading Scientific Schools of Russia." The author thanks A.M. Cherepashchuk, E.A. Antokhina, and V.M. Lipunov for useful discussions and advice, as well as Dr. G. Hammerschlag-Hensberge, who kindly presented his spectral data for this study.

#### REFERENCES

1. C. Jones *et al.*, *Astrophys. J.* **781**, 64 (1973).
2. C. Jones *et al.*, *Bull. Am. Astron. Soc.* **5**, 313 (3972).
3. C. Jones and W. Lillei, *IAU Circ.*, № 2503 (1973).
4. A. P. Reynolds *et al.*, *Astron. Astrophys.* **359**, 873 (1999).
5. L. Kaper and A. Cherepashchuk, in *Black Holes in Binaries and Galactic Nuclear: Diagnostic, Demography and Formation*, Ed. by L. Kaper, E. P. J. van Heuvel, and P. A. Noudt (Springer, Berlin, 2006), p. 289.
6. J. B. Hutchings, A. D. Thackeray, B. L. Webster, and P. J. Andrews, *Mon. Not. R. Astron. Soc.* **163**, 13 (1073).
7. S. R. Heap and M. F. Corcoran, *Astrophys. J.* **887**, 390 (1992).
8. R. G. Aitken, *The Binary Stars* (Dover, New York, 1964).
9. P. S. Conti and A. P. Cowley, *Astrophys. J.* **200**, 133 (1975).
10. C. Jones *et al.*, *Astrophys. J.* **459**, 259 (1996).
11. J. S. Clark *et al.*, *Astron. Astrophys.* **392**, 909 (2002).
12. G. Hammerschlag-Hensberge, C. De Loore, and van Den Heuvel, *Astron. Astrophys.*, Suppl. Ser. **32**, 375 (1978).
13. G. Hammerschlag-Hensberge, M. H. van Kerkwijk, and L. Kaper, *Astron. Astrophys.* (in press).
14. J. B. Hutchings, *Astrophys. J.* **235**, 413 (1980).
15. D. Crampton, J. B. Hutchings, and A. P. Cowley, *Astrophys. J.* **299**, 839 (1985).
16. ??H. Quantrell, A. J. Norton, T. D. C. Ash, *et al.*, *Astron. Astrophys.* (2003) (in press).
17. A. V. Goncharskiĭ, S. Yu. Romanov, and A. M. Cherepashchuk, *Finite-Parametric Inverse Problems* (Izd-vo Mosk. Gos. Univ., Moscow, 1991), pp. 107, 99 [in Russian].
18. E. A. Antokhina and A. M. Cherepashchuk, *Astron. Zh.* **71**, 420 (1994) [*Astron. Rep.* **38**, 367 (1994)??].
19. E. A. Antokhina, *Astron. Zh.* **73**, 532 (1996) [*Astron. Rep.* **40**, 483 (1996)].
20. A. A. Rubashevskiĭ, *Astron. Zh.* **68**, 799 (1991) [*Sov. Astron.* **35**, 626 (1991)].
21. D. Hudson, *Statistics. Lectures on Elementary Statistics and Probability* (Geneva, 1964; Mir, Moscow, 1970).
22. M. Milgrom, *Astron. Astrophys.* **70**, 763 (1978).
23. M. K. Abubekero, E. A. Antokhina, and A. M. Cherepashchuk, *Astron. Zh.* **81**, 1 (2004) [*Astron. Rep.* **48**, 89 (2004)].
24. A. Herrero, *IAU Symposium № 212: A Massive Star Odyssey: from Main Sequence to Supernova*, Ed. by K. van der Hucht, A. Herrero, C. Esteban (Publ. Astron. Soc. Pac., 2003), p. 3.
25. J. Ziolkowski, *Nonstationary Evolution of Close Binaries* Ed. by A. N. Zitkov (PWN, Warsaw, 1978), p. 29.
26. A. M. Cherepashchuk, N. A. Katysheva, Khruzina, and C. Yu. Shugarov, *Highly Evolved Close Binary Stars: Catalog* (Netherland Gordon and Breach Sci., 1996), Vol. 1, Part 1, p. 82.
27. M. H. van Kerkwijk, J. van Paradijs, and E. J. Zuiderwijk, *Astron. Astrophys.* **303**, 497 (1995).
28. S. E. Thoresett and D. Chakrabarty, *Astrophys. J.* **512**, 288 (1998).

*Translated by D. Gabuzda*